Figure S1 – Gemcitabine resistant cells are enriched for CSCs. (**A**) Flow cytometry for surface expression of CD133, SSEA1, and CXCR4 in Gemcitabine resistant cells versus control cells. (**B**) QPCR analysis of pluripotency-associated genes (**left panel**) and genes related to EMT (**right panel**). (**C**) QPCR analysis for expression of TGFBR2, ALK4, SMAD2, SMAD4, and TBX3 in gemcitabine resistant cells versus control cells. (**D**) QPCR analysis for the expression of ABC transporters (ABCC1 and ABCG2) and Gemcitabine transporters (hENT1, hENT2, hCNT1, and hCNT3) in gemcitabine resistant cells versus control cells. Data are normalized for ß-Actin expression. (**E**) Flow cytometry analysis of gemcitabine treated tumors depleted by MACS for mouse CD45 and mouse CD146**.**

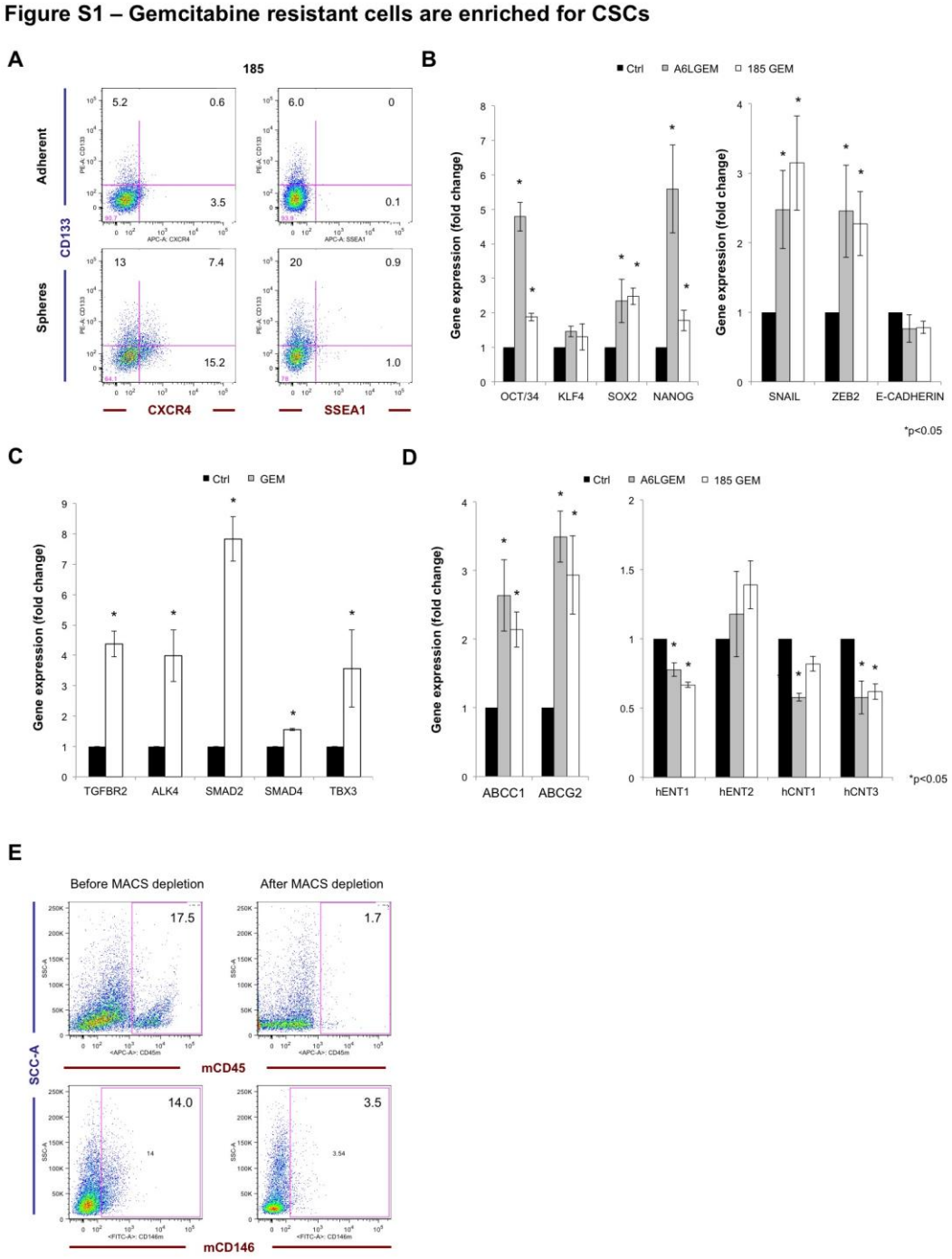

Figure S2 – Slow cycling cells possess CSC phenotype. (**A**) Flow cytometry for surface expression of CD133, SSEA1, and CXCR4 in PKH26+ and PKH26– cells, respectively (**B**) Sphere formation capacity of PKH26+ versus PKH26– cells isolated from A6l, 253, and 354 PDAC tumors (n=3; *P<0.05).

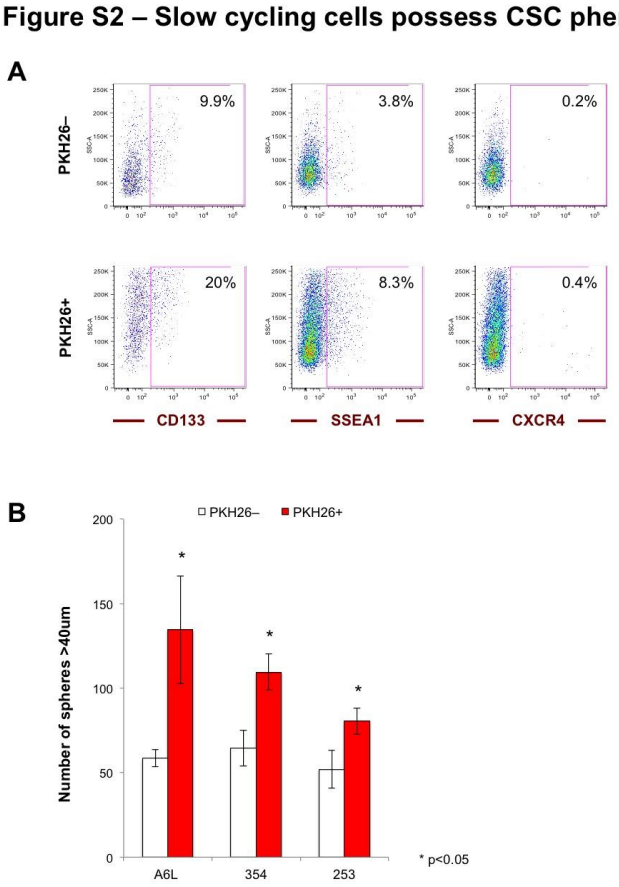

Figure S3 – miR-17-92 downregulation in spheres and in gemcitabine resistant cells. (**A**) QPCR analysis for the expression of miR-17-92 family members in Gemcitabine resistant cells and spheres versus respective control cells. (**B**) QPCR analysis for the expression of miR-17-92 family members in PKH26+ and PKH26– cells isolated from 185 and 354 PDAC tumors. (**C**) Western blot analysis for the expression of the cell cycle regulator p21 in adherent cells treated with antagomir-17-92 versus antagomir-Ctrl. (**D**) *In vivo* tumorigenicity of A6L and 185 treated with antagomir-17-92 versus antagomir-Ctrl.

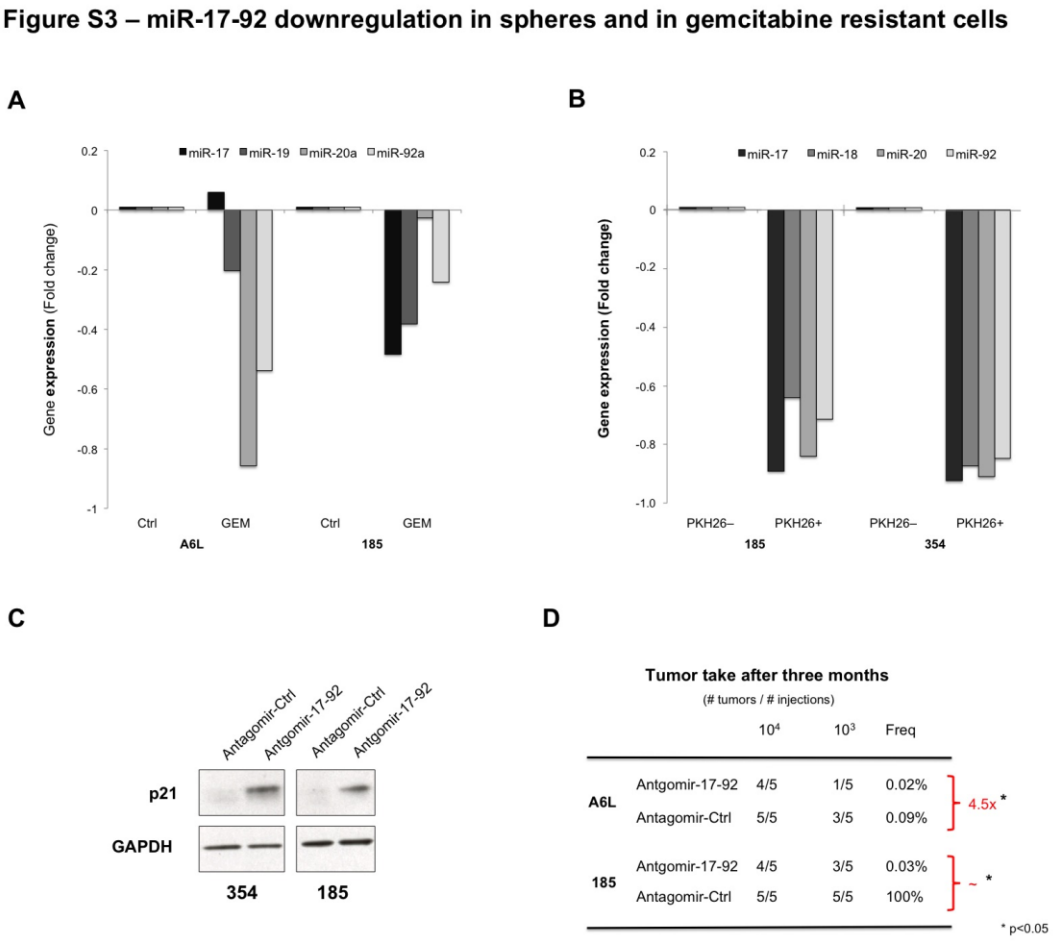

Figure S4 – miR-17-92 overexpression impairs CSC phenotype. (**A**) Lentiviral overexpression of miR-17-92 in CSCs. Representative images of GFP expression post infection (**upper panel**), illustration of the utilized sorting strategy (**middle panel**), and qPCR analysis for the expression of miR-17-92 family members in GFP sorted cells (**lower panel**). (**B**) QPCR analysis for the expression of pluripotency-associated genes in miR-17-92 cells versus miR-Ctrl cells. (**C**) Representative images for ß-galactosidase staining in miR-17-92 cells versus miR-Ctrl cells. (**D**) Percentage of PKH26+ cells over a period of 4 weeks in miR-17-92 cells versus miR-Ctrl. (**E**) Sphere counts during serial *in vivo* passaging of miR-17-92 cells versus miR-Ctrl cells. (**F**) Cell cycle analysis using Ki67 and DAPI of cell freshly isolated cells after serial *in vivo* passaging. (**G**) Quantification of migratory activity in the wound-healing assay with stimulation of TGF-ß1 or NODAL in the presence or absence of the ALK4,5,7 inhibitor SB 431502.

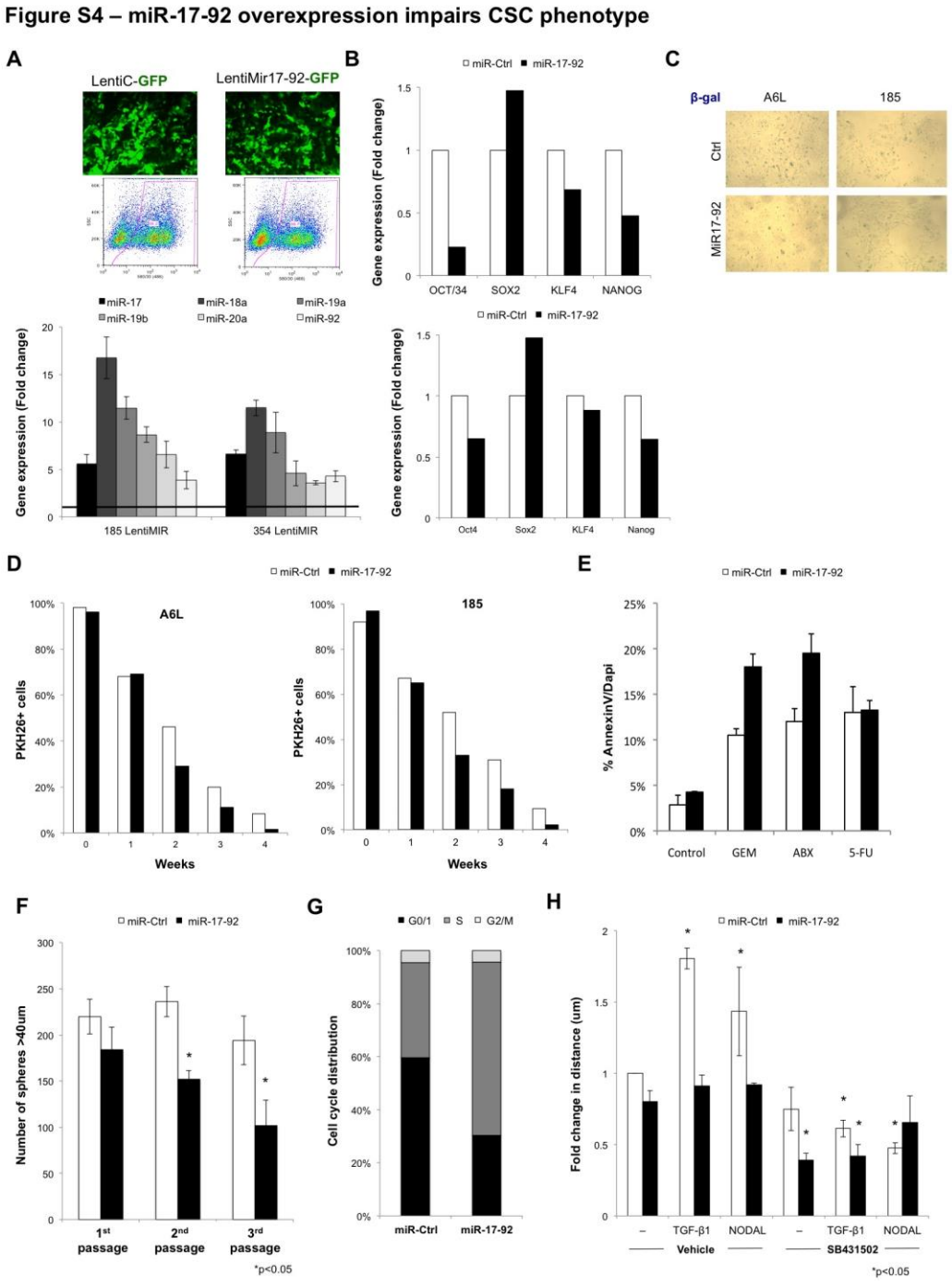

Figure S5 – miR-17-92 target multiple members of NODAL/TGF-ß1 signaling. (**A**) Sequence alignment of miR-17-92 family members' seed sequence in *TGFBR2* 3′ UTR, *ALK4* 3′ UTR, *SMAD2* 3′ UTR, *SMAD4* 3′ UTR, *p21* 3′ UTR, *p57* 3′ UTR, and *TBX3* 3′ UTR. (**B**) QPCR analysis for the expression of miR-17-92 family members 96h after induction with Doxycycline. (**C**) RTqPCR analysis of miR-17-92 target genes after 24h of treatment with single antagomirs against each of the six members of the miR-17-92 cluster.

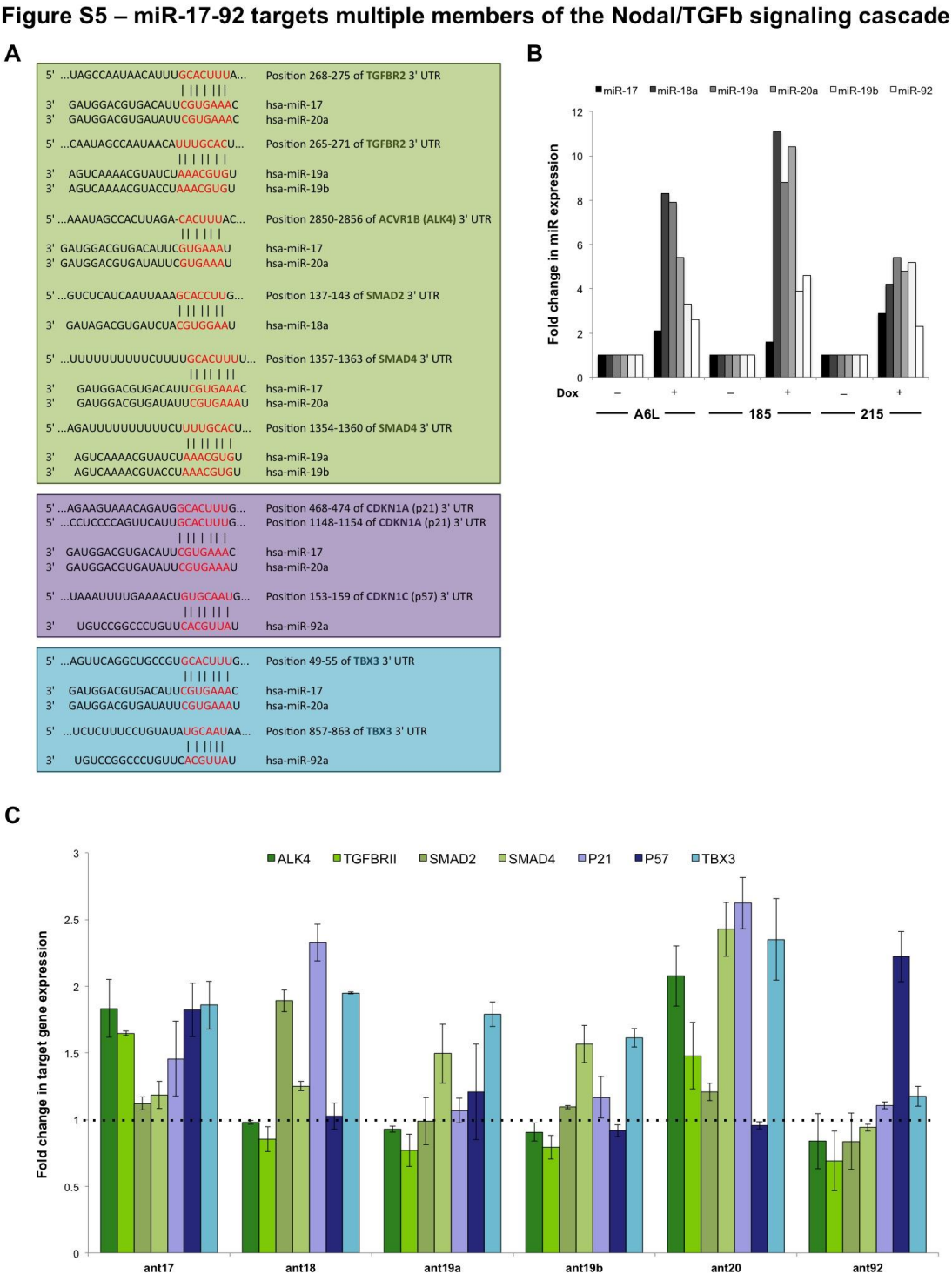

Figure S6 – Knockdown of p21 or TBX3 inhibits cancer stem cell phenotype. (**A**) Representative images of invaded cells **(left panel).** Percentage of invading cells (Ctrl versus sh-p21) through Matrigel™ following stimulation with FBS, NODAL or TGF-ß1 **(right panel**). (**B**) RTqPCR analysis of TBX3 mRNA levels in multiple PDAC sphere cultures (s) compared to their respective adherent controls (n = 3; *p < 0.05). (**C**) Western blot analysis for the expression of TBX3 in cells sorted for CD133 surface expression (**upper panel**) and densitometric quantification of the western blot (**lower panel**). (**D**) QPCR analysis for the expression of TBX3 in cells sorted for ALK4 surface expression. (**E**) Percentage of invading cells through Matrigel™ following stimulation with NODAL, ACTIVIN or TGF-ß1 (n = 3; *p < 0.05).

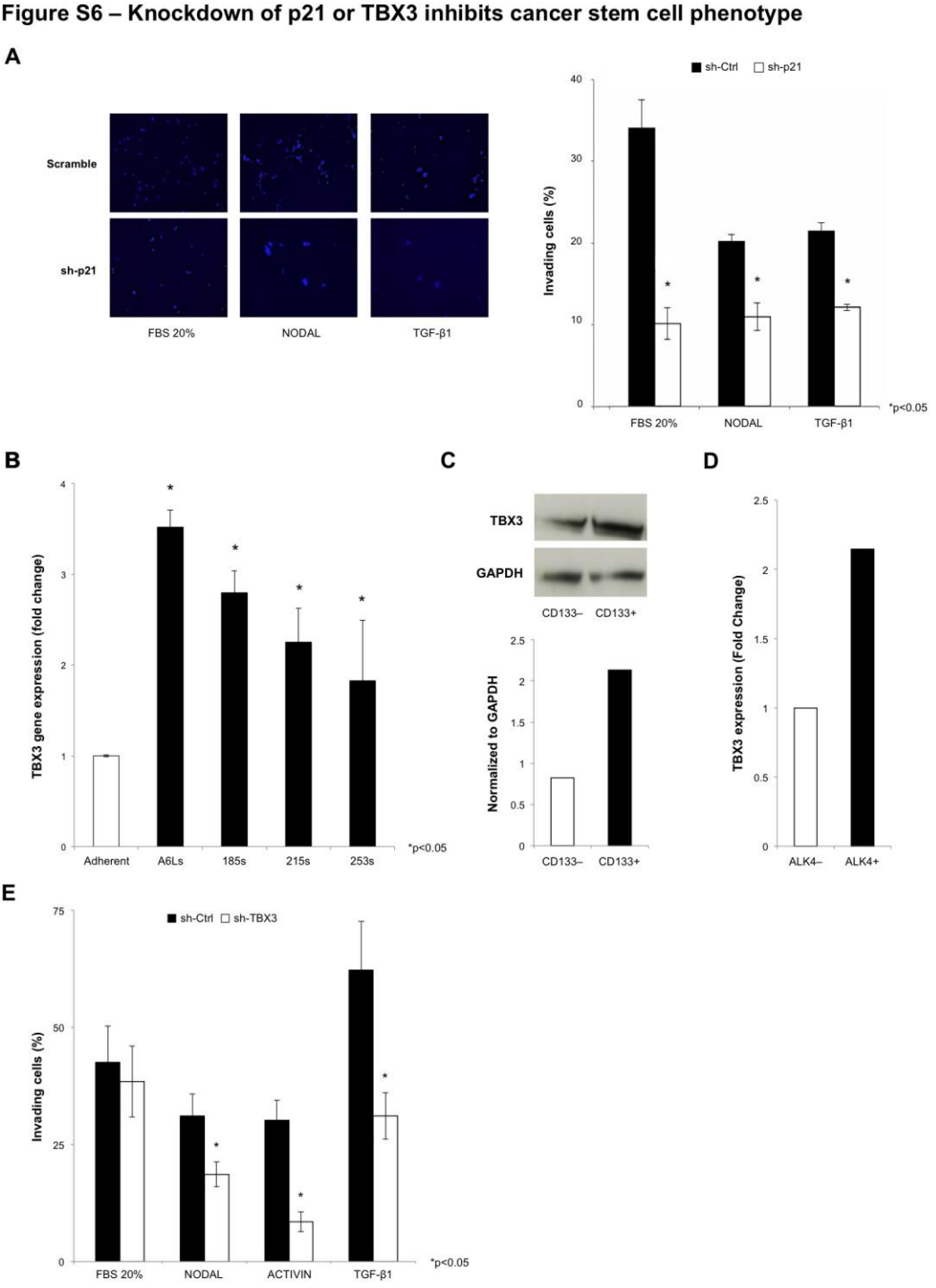

Figure S7: *In vivo* overexpression of miR-17-92 reverses quiescence and chemoresistance.
Treatment effects of gemcitabine and abraxaen in miR-17-92 overexpressing cells in established tumors derived from **(A)** A6L and (**B**) 185 cells, respectively, in immunocompromised mice. The mean tumor volume is given; n 6 tumors per group. P value was determined by Student t test.